This is a repository copy of *Spectral Analysis of Short-Time Biomedical Data Using Adaptive Filters*.

White Rose Research Online URL for this paper:
http://eprints.whiterose.ac.uk/76358/

Monograph:
Braham Levy, J and Linkens, D. A. (1983) Spectral Analysis of Short-Time Biomedical Data Using Adaptive Filters. Research Report. ACSE Report 218 . Department of Control Engineering, University of Sheffield, Mappin Street, Sheffield

SPECTRAL ANALYSIS OF SHORT-TIME BIOMEDICAL

DATA USING ADAPTIVE FILTERS

by

J. Braham Levy, B.Sc., M.Eng.[*] and

D.A. Linkens, B.Sc., (Eng.), M.Sc., Ph.D., C.Eng., MIEE

Department of Control Engineering,
University of Sheffield,
Mappin Street, Sheffield S1 3JD.

[*] formerly as above, now; Lucas Research Centre, Shirley, W. Midlands.

ABSTRACT

Conventional methods of spectral analysis are unable to track small but rapid, variations in frequency. The LMS algorithm used as an adaptive line enhancer is found to track these signals, and provides insight into mechanical and physiological effects of the human body when analysing electrical signals obtained from internally and externally placed electrodes.

1. Introduction

Spectral Analysis of biomedical signals is of considerable interest in the investigation and understanding of the workings of human physiology. The detection and resolution of frequencies which may be time-varying, due to mechanical actions correlated to the electrical signals of the body, is a major motivation for this analysis.

The analysis can be done by many methods, the standard ones being that of Fourier Transforms and associated techniques. These methods have a major drawback in that they require large quantities of data to produce significant results. As a result, any variation in frequency, or perturbation, can be smoothed out by the action of the algorithm, e.g. the FFT where it will appear as a 'broad' spectral peak centred at the frequency of interest, particularly if using zero padding.

As data from human patients cannot usually be obtained for long times analysis methods using shorter-time-series are sought. This has the double effect of being able to track any variation in frequency which occurs, and can be performed over a shorter time than that required for say an FFT.

Following earlier work in adaptive array systems (1) and geophysics(2) a whole set of algorithms has been used (3) to resolve these problems, the most attractive being that of Autoregressive (AR) Spectral Analysis. These methods have not only been applied to biomedical signals, as mentioned above, but also a wealth of different algorithms have been developed producing singificant results, full and detailed descriptions of which can be found in several recent publications e.g. (3).

In this study an early developed algorithm, the least mean squares (LMS) gradient search method (4) has been used to provide real-time analysis of biomedical data from both the human gastro-intestinal tract

and processed ECG signals providing so-called heart rate variability
(HRV) time series.

2.   The LMS Algorithm

Developed in the early 60's by Widrow et al the advantage of this
algorithm lies in its computational simplicity and ease of guaranteed
convergence.

Consider the prediction of a data point from solely past data

$$\hat{x}(k) = \sum_{\ell=1}^{P} a_\ell(k)x(k-\ell) \qquad (2.1)$$

where x(m) is the data series

$\{a_m(k)\}$ is a coefficient weighting vector $m=1,2\ldots P$

applied to $\{x(m)\}$

and

$$e(k) = x(k) - \hat{x}(k) \qquad (2.2)$$

where e(k) is the prediction error. Considering the minimization of
$e^2(k)$

$$\min\left[e^2(k)\right] = \min\left[\{x(k) - \hat{x}(k)\}^2\right] \qquad (2.3)$$

by performing this minimization we will obtain the set of coefficients,
a_ℓ^* $\ell = 1,2\ldots P$ which are optimal in the mean-square sense. Thus
taking expected values

$$E\left[e^2(k)\right] = E\{\left[x(k) - \hat{x}(k)\right]^2\} \qquad (2.4)$$

and rewriting in vector notation 2.1 becomes

$$\hat{x}(k) = X_k^T A_k = A_k^T X_k \qquad (2.5)$$

where $X_k^T = \begin{pmatrix} x(k-1) \\ x(k-2) \\ . \\ . \\ . \\ x(k-P) \end{pmatrix}$

$\qquad (2.6)$

i.e. a vector of past data

$$A_k = \left[a_1(k), a_2(k), \ldots a_p(k) \right] \tag{2.7}$$

the coefficient vector.

Thus (2.4) now becomes

$$E\left[e^2(k) \right] = E\left[x^2(k) \right] - 2 E\left[x(k) \ X_k^T \right] A_k$$

$$+ A_k^T E\left[X_k X_k^T \right] A_k \tag{2.8}$$

and by defining

$$P_k \triangleq E\left[x(k) \ X_k^T \right] = E \begin{pmatrix} x(k) \ x(k-1) \\ x(k) \ x(k-2) \\ \cdot \\ \cdot \\ \cdot \\ x(k) \ x(k-P) \end{pmatrix} \tag{2.9}$$

which can be seen to be an autocorrelation vector, and

$$R_k \triangleq E\left[X_k X_k^T \right] = E \begin{pmatrix} x(k-1) \ x(k-2) \ \ldots \ldots \\ x(k-2) \ x(k-2) \\ \cdot \\ \cdot \\ \cdot \\ x(k-P) \ x(k-P) \ \cdot \cdot \cdot \cdot \cdot \end{pmatrix} \tag{2.10}$$

which is an autocorrelation matrix

Thus we can rewrite (2.8) as

$$E\left[e^2(k) \right] = E\left[x^2(k) \right] - 2P_k^T A_k + A_k^T R_k A_k \tag{2.11}$$

which can be seen to be a quadratic function in the coefficient vector A_k.

Taking the gradient of (2.11) w.r.t. A_k

$$\nabla_k = - 2P_k + 2R_k A_k \tag{2.12}$$

and by setting (2.11) to zero we obtain the optimum, Weiner, coefficient

vector

$$A_k^* = R_k^{-1} P_k \tag{2.13}$$

The LMS algorithm uses the method of steepest descent so that the coeffi-

cient vector A_k is updated by a change proportional to the negative

gradient $- \nabla_k$.

$$A_{k+1} = A_k - \mu \nabla_k \tag{2.14}$$

An expression for the gradient can be found to be

$$\hat{\nabla}_k = -2 \, e(k) \, X_k \tag{2.15}$$

and so the LMS algorithm is given by

$$A_{k+1} = A_k + 2 \, \mu e(k) \, X_k \tag{2.16}$$

where μ is a step size and determines the convergence of the algorithm. It has been shown (1) that convergence is guaranteed by setting

$$\frac{1}{\lambda_{max}} > \mu > 0 \tag{2.17}$$

where λ_{max} is the largest eigenvalue of the Toeplitz matrix R_k. It has further been shown (5) that

$$\frac{2}{r_x(o)p} > \mu > 0 \tag{2.18}$$

where $r_x(o) = \dfrac{1}{P} \sum_{\ell=1}^{P} x(k) \, x(k) = \sigma^2 \tag{2.19}$

i.e. the signal power.

The predictor can now be viewed as an all pole adaptive filter taking data $\{x(m)\}$ and producing a white output $\{e(m)\}$. (The output will be white if the prediction is essentially correct).

The transfer function of this filter is thus an estimate of the PSD of the signal

$$Q(\omega,k) = \frac{\sigma^2}{\left| 1 - X_k^T A_k \right|^2} \tag{2.20}$$

A simpler estimate which omits absolute gain knowledge but preserves frequency information is given (5) by

$$\hat{Q}(\omega,k) = \frac{1}{\left| 1 - X_k^T A_k \right|^2} \tag{2.21a}$$

$$= \frac{1}{\left| 1 - \sum_{\ell=1}^{P} a_\ell(k) x(k-\ell) \right|^2} \tag{2.21b}$$

The denominator of (2.21b) can be evaluated simply by a zero padded FFT yielding a **correct** result (no biasing) as all the information required is contained within the data length of the FFT; the AR adaptive filter coefficients can be viewed as forming an impulse response. This is then the Adaptive Line Enhancer (ALE) (1).

3. Methods

It can be seen that the LMS algorithm has considerable computational simplicity and is thus suitable for implementation on a real-time micro-processor system. To this end a Texas Instrument FS990/4 Development System, based around a TMS9900 16-bit microprocessor, incorporating 28K words of memory, Analog to Digital and Digital to Analog convertors (Analog Devices RTS-124X series) was employed. As a programming language Texas Instruments Microprocessor Pascal (TIMPP) was chosen, the reasons for this choice being three fold.

(i) Very high speed of operation is not essential with the particular biomedical signals being used, sample periods being as low as 1 second, hence a high level language can be used for the obvious reason that the development time to produce a working system is less.

(ii) TI MPP has its own real-time operating system which allows 'concurrent' programming. This allows the LMS algorithm to proceed every sample, the ALE operation i.e. FFT on the zero padded coefficients produced by the LMS algorithm and display of such, at a different slower rate, and a user interaction process for the control of the overall system, to appear to be all happening simultaneously i.e. concurrently. (see Fig. 1).

(iii) The authors preference for the Pascal Programming Language (6).

Digestive tract data were gathered from internal electrodes stitched to the sevosal wall of the stomach and duodenum, and also from Ag/AgCl electrodes (as used in heart beat monitoring) on the surface of the abdomen.

The HRV data were obtained from ECG signals which were processed to an analog form to give a 'beat-to-beat' variability signal. The resulting variability was synchornized by an external thermal stimulus applied to the patient at a set frequency.

4. Results

The results are shown graphically in figures 2 through 16. These graphs are two dimensional representations of three dimensional data thus:-

frequency is traversed along the horizontal axis while time (iteration number) along the vertical axis. The triangles represent significant amplitude peaks in the ALE.

The graphs were obtained from either a Tektronix 4010 terminal or from a Hewlett-Packard 7225A plotter. Figures 2 and 3 show results obtained from human duodenum data. In figure 2 a clear frequency component at 0.2Hz is seen as is one at 0.4Hz. 0.2Hz is known to be the electrical frequency of the duodenum and superimposed on this can be seen the perturbations, due to mechanical actions, occuring over 2-3 cycles of data. The tracking of this signal is particularly good due to its near sinusoidal waveform and high signal-to-noise ratio. The tracked 0.4Hz component is the second harmonic of the duodenum 0.2Hz signal. In Figure 3 again clear tracking at 0.2Hz is seen with very large perturbations in frequency at several points lasting for 2-3 cycles of data. No harmonic is detected here but a subharmonic component (0.1Hz) is apparent as is a signal at 0.3Hz likely to be due to respiration of the patient. The 0.1Hz component is possibly a beat frequency between

the duodenum and respiratory frequencies. Results from external elec-
trodes on the abdomen are shown in figures 4-7. A sample of the input
data to the algorithm from a surface recording is shown in figure 4 with
an FFT performed on this data length (512 points = 8 mins 32 seconds
of data) it can be seen from the FFT that a clear frequency component
of 0.05Hz is detected as are minor peaks, due to the fluctuations in
this frequency, on either side. Only a small second harmonic component
is shown on the FFT due to the scaling of the graph. Figure 5 shows the
ALE performed on the same data. Clearly a frequency of 0.05Hz is
detected known to be the frequency of the human slow-wave as are harmonics at
0.1, 0.15 and 0.2Hz. Some breakthrough of respiration is seen later
in the graph at 0.3Hz, as is a very low frequency component probably
due to thermal effects, which is also seen on the FFT. Perturbations in
the 0.05Hz signal lasting 2-3 cycles are clearly seen on the ALE,
but are not visible on the FFT.

Figures 6 and 7 show the ALE performed on the similar data using
different lengths of adaptive filter. Again the 0.05Hz signal is clearly
detected along with harmonics, as are the perturbations due to the
previously mentioned mechanical activity. The large number of extra-
neous peaks at the beginning of the plot shows the adaptive algorithm
'tuning' due to a fairly low signal-to-noise ratio.

Figures 8 and 9 again show similar results on the data from a different
patient for different filter lengths.

Figures 10 and 11 show spectacularly how the ALE can go wrong!
Figure 12 shows a sample waveform of the recording used for these graphs
and which was produced from internal electrodes stitched to the
servosal surface of the gut. The signal is quite clearly rich in har-
monic content as can be seen on the associated FFT. The ALE in
attempting to detect these frequencies produces spurious frequency com-

ponents in the ALE.

Figures 13 - 16 show ALE graphs performed on Heart Rate Variability data, at external thermal stimulus frequencies of 0.025 Hz, 0.05HZ, 0.07 and 0.1 Hz respectively. Figures 13, 14, and 16 show clearly the basic 0.1Hz HRV signal modulated by the stimulus frequency. The failure of Fig. 15 to track clearly is due to the frequency of the stimulus not being harmonically related to the basic 0.1 Hz rhythm. Occasional breakthrough of respiration at 0.3Hz is seen in all these graphs. These results agree with those produced by Kitney (7) using running low-pass filtered event series (LPFES) spectra.

4. Conclusions

The ALE is particuluarly good at detecting sinusoids in white noise and to some extent coloured noise. When the noise is harmonically rich viz. figures 10, 11 (the signal harmonics can be regarded as noise here) the ALE breaks down, as has been shown, as a tracker of the major, predominant frequency. Other effects of noise can be seen in start-up transients viz. fig. 6,7 during the adaptive tuning period. Both of these can be viewed in the following way initially the all pole filter will attempt to place its poles equally around the unit circle in the z-plane. As tuning continues and the signal is detected those poles due to the noise migrate away from the unit circle and thus become less and less significant. With harmonically rich signals. This does not happen as there is essentially no one predominant frequency.

The choice of model order, P, and the convergence rate determined by μ the search step size affects the results obtained. Empirical rules (8) seen to be born out by practical examples although recently (9),(10) an attempt has been made to quantify this for the lattice filter ALE. These results although apparently good for pure sinusoids plus white noise do not work for the biomedical signals under investigation here.

when applied to the LMS/ALE combination. The quantification of choice of model order, P, still has some way to go, and for the present empirical rules seem adequate to produce good results.

As for μ, which determines the convergence of the algorithm. This can be decided using a modification of the inequality (2.18)

$$\mu_k = \frac{\alpha}{r_x(o)P} \qquad (4.1)$$

$$0 < \alpha < 2 \qquad (4.2)$$

where μ is adapted continuously on line dependent on α - a user entered parameter and $r_x(o)$. The signal power can be estimated on-line by several methods one such being

$$\sigma^2(k) = \sigma^2(k-1) + (1-\mu)\ \sigma^2(k) \qquad (4.3)$$

$$\sigma^2 = r_x(o)$$

The authors however prefer to use a sliding window method which estimates $\sigma^2(k)$ using the past model order number of samples by equation (2.19). This can be viewed as a fixed length-moving filter whereas (4.3) is essentially a low-pass filter. Both methods will track variations in signal power strength, essential in real-time signal processing. The method used is one of personal choice.

The time to adaption is governed by μ and hence in our case α, and it has been shown that the adaptive time, τ_a, is given approxmately (5) by

$$\tau_a \simeq \frac{-1}{\ln(1-\mu\lambda_{avg})} \qquad (4.4)$$

where λ_{avg} is the average eigenvalue in the matrix R_{xx} this is equivalent to

$$\tau_a \simeq \frac{-1}{\ln(1-\alpha/P)} \qquad \text{where } 0 < \alpha < 2. \qquad (4.5)$$

This on-line computation of μ given α greatly aids the robustness of the

LMS/ALE algorithm by always guaranteeing the convergence within a set time as can be seen from the results.

The use of the LMS/ALE algorithm in real-time operation given the results shown above leads to a possible clinical application in post-operative care of patients (11) who have undergone abdominal surgery. A portable system incorporating graphical display would aid greatly in the detection of migrating myoelectrical complexes (MMC's) occurring in the stomach using surface and/or serosal electrodes, thus indicating a return to normal electrical patterns of behaviour.

The use of the LMS/ALE algorithm on HRV signals should also aid in the study of Thermoregulatory and other influences on heart-rate variability where work may be done on-line instead of the present off-line work (7). Use has also been made of   spectral analysis for the study of Reynauld's disease (12), a particularly disabling disease of the cir-culatory system of humans. On-line analysis by the LMS/ALE should be able to detect this problem easily and quickly and also aid in monitoring its progress under treatment. Further use of the LMS algorithm has been made in obtaining parameter estimates for control systems in for example adaptive or optimal control schemes (13). The inherent simplicity and robustness of the algorithm should produce control algorithms which could easily be continuously adapted.
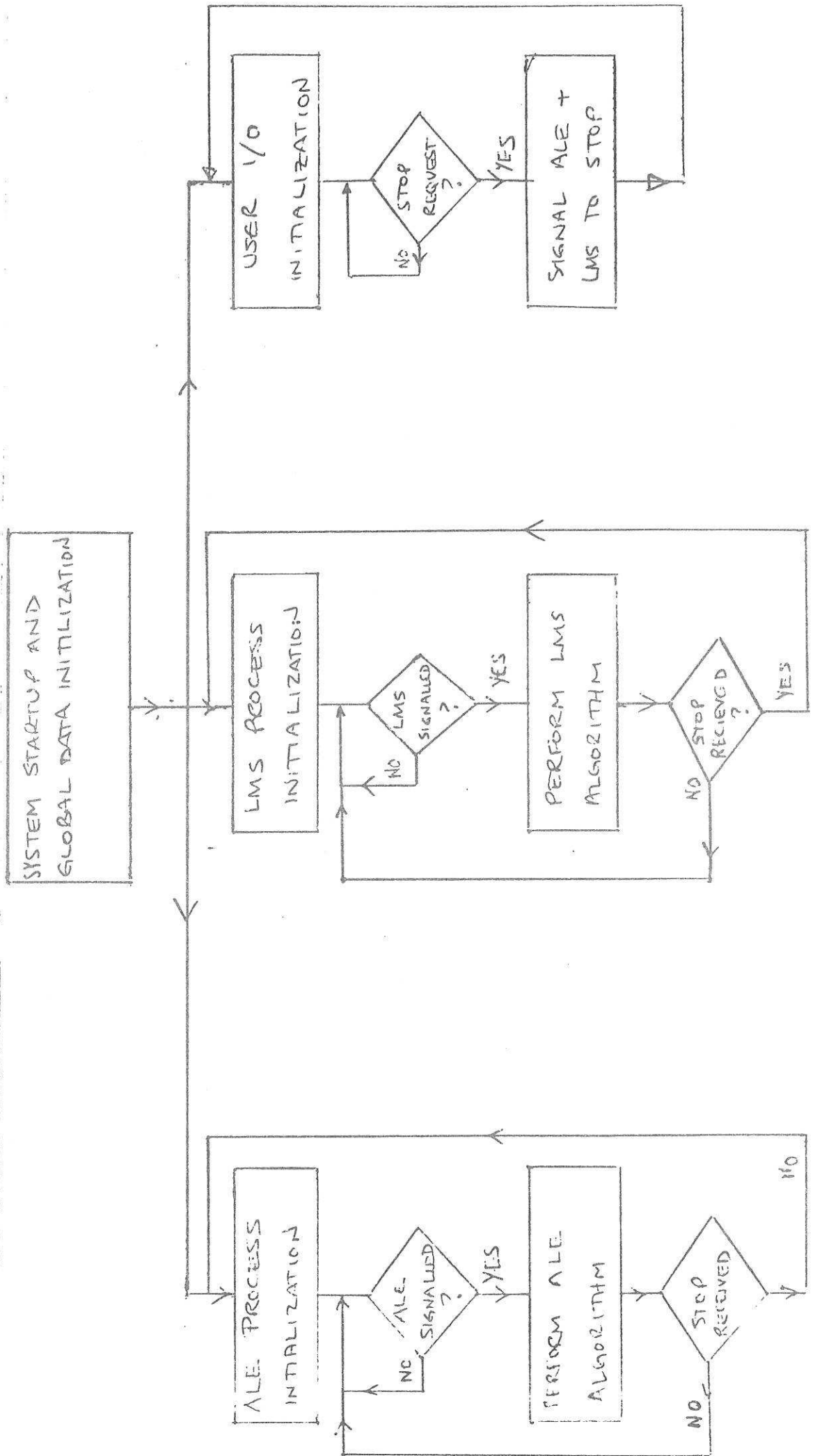
5. Acknowledgements

6. References

1. Widrow, B, et al, Adaptive Noise Cancelling, Proc. IEEE, 63, 12,

    pp. 1692-1716, December 1975.

2. Burg, Maximum Entropy Spectral Analysis, in Proc. 37th Meeting of

    Society of Explorations Geophysicists, pp. 34-41, October 1967.

3. Kay and Marple, S.L., Spectrum Analysis - A Modern Perspective, Proc.

    IEEE, 69, pp. 1380-1419, 1981.

4. Widrow, B., Adaptive Filters 1: Fundamentals, Stanford University,

    Tech. Rep. No. 6764-6, SU-SEL-66-126, December 1966.

5. Griffith, L.J., The Rapid Measurement of Digital Instantaneous

    Frequency, IEEE Trans. ASSP-23, pp. 207-222, April 1975.

6. Jensen, K. and Wirth, N., Pascal User Manual and Report 2nd edition,

    Springer-Verlag, 1975.

7. Kitney, R.I. and Rompleman, O., (Eds), The study of heart-rate variability.

    Oxford University Press.

8. Linkens, D.A., Empirical rules for the selection of parameters for auto-
    regressive spectral analysis of biomedical rhythms. Signal Processing,
    Vol. 1, No. 4, pp. 243-258, 1979.

9. Reddy, V.U., Egardt, B., and Kailath, T., Optimized lattice-form

    Adaptive line Enhancer for a Sinusoidal Signal in Broad-Band Noise,

    IEEE Trans. ASSP-29, 3, pp. 702-709, June 1981.

10. Zeidler et al, Adaptive Enhancement of multiple sinusoids in uncorrelated

    noise, IEEE Trans. ASSP-26, pp. 240-254, June 1978.

11. Levy, J.B., Linkens, D.A., Rimmer, S.R., Johnson, A., Stoddart, C.J.,
    Adaptive tracking of human slow-wave frequency changes using surface
    and serosal signals.

    In Proc. 1st European Symposium on Gastrointestinal Mobility Bologna,

    Italy, September 1982.

12. de Trafford et al, 'Modelling of the human vasomotor control system and its application to the investigation of arterial disease', Proc. IEE, vol. 129, Pt. A., No. 9 December 1982, pp. 646-650.

13. Bitmead, R.R., Covergence in Distribution of LMS-type Adaptive Parameter Estimates, IEEE Trans. Automatic Control, Vol. AC-28, 1, pp. 54-60, January 1983.

Figure Captions

1. Flow chart for concurrent PASCAL adaptive filtering programms.

2. ALE tracking on serosal duodenal recording for subject H.

3. ALE tracking on serosal duodenal recording for subject D.

4. Time series data and FFT for surface recording for subject P.

5. ALE tracking for surface recording from subject P.

6. ALE tracking for surface recording from subject H. using 25th order filter.

7. ALE tracking data for Fig. 6 with 19th order filter.

8. ALE tracking for surface recording from subject D using 25th order filter.

9. ALE tracking data from Fig. 8 with 19th order filter.

10. Incorrect tracking of serosal gastric recording from subject H2.

11. Incorrect tracking of serosal gastric recording from subject D.

12. Time series data and FFT for serosal gastric recording from subject H2.

13. ALE tracking of heart rate variability data from patient GC thermally stimulated at a frequency of 0.025 Hz.

14. ALE tracking as for Fig. 13 but stimulus frequency of 0.05 Hz.

15. ALE tracking as for Fig. 31 but stimulus frequency of 0.07 Hz.

16. ALE tracking as for Fig. 13 but stimulus frequency of 0.1 Hz.

CONCURRENT OPERATION FLOWCHART - ALL THREE PROCESSES APPEAR TO RUN SIMULTANEOUSLY

Fig 1

Center process (top to bottom):
- SYSTEM STARTUP AND GLOBAL DATA INITIALIZATION
- LMS PROCESS INITIALIZATION
- LMS SIGNALLED? — NO (loop back) / YES
- PERFORM LMS ALGORITHM
- STOP RECIEVG D? — NO (loop back) / YES

Left process (top to bottom):
- ALE PROCESS INITIALIZATION
- ALE SIGNALLED? — NO (loop back) / YES
- PERFORM ALE ALGORITHM
- STOP RECIEVED — NO / YES

Right process (top to bottom):
- USER I/O INITIALIZATION
- STOP REQUEST? — NO (loop back) / YES
- SIGNAL ALE + LMS TO STOP
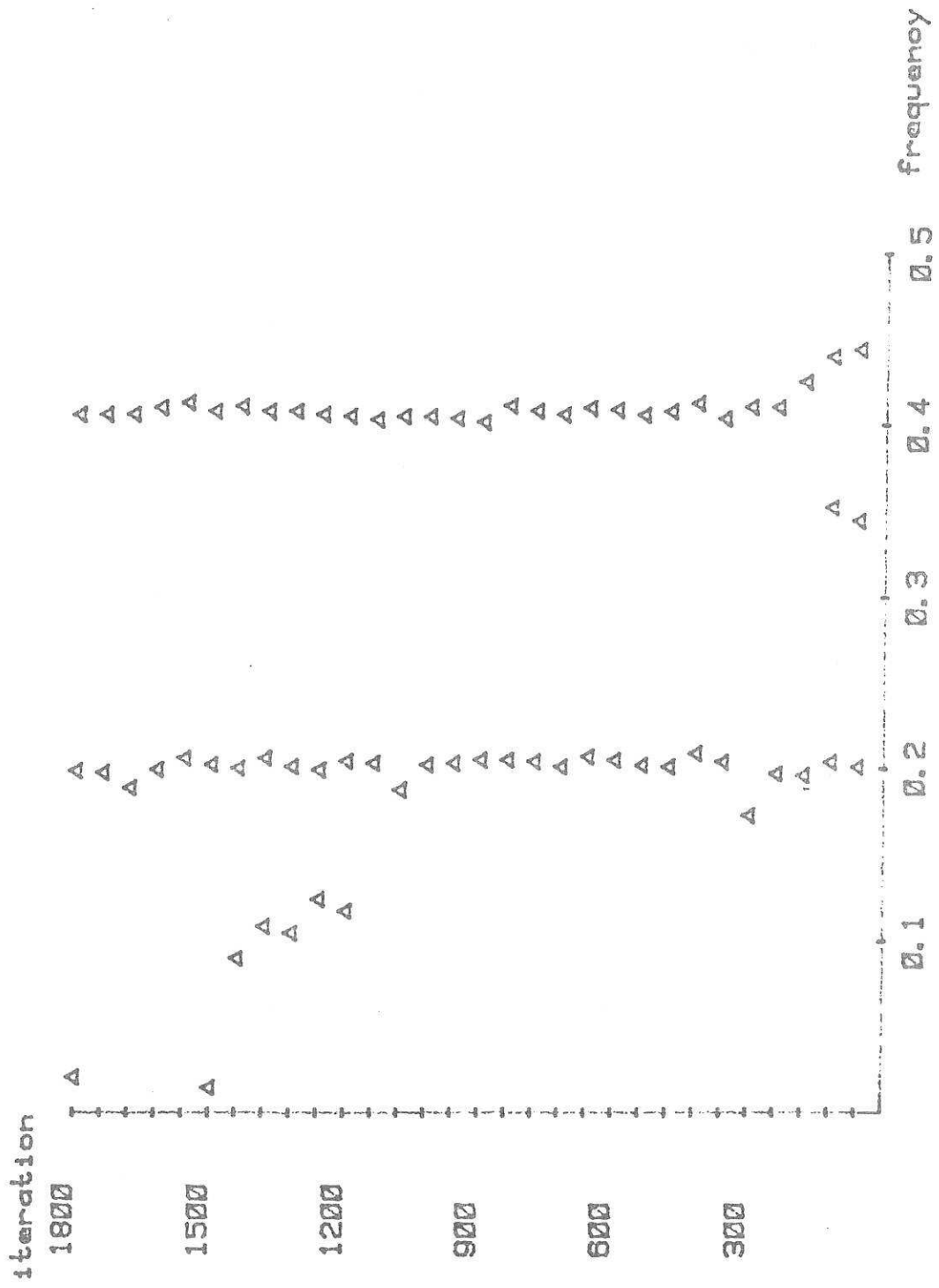
Fig. 2
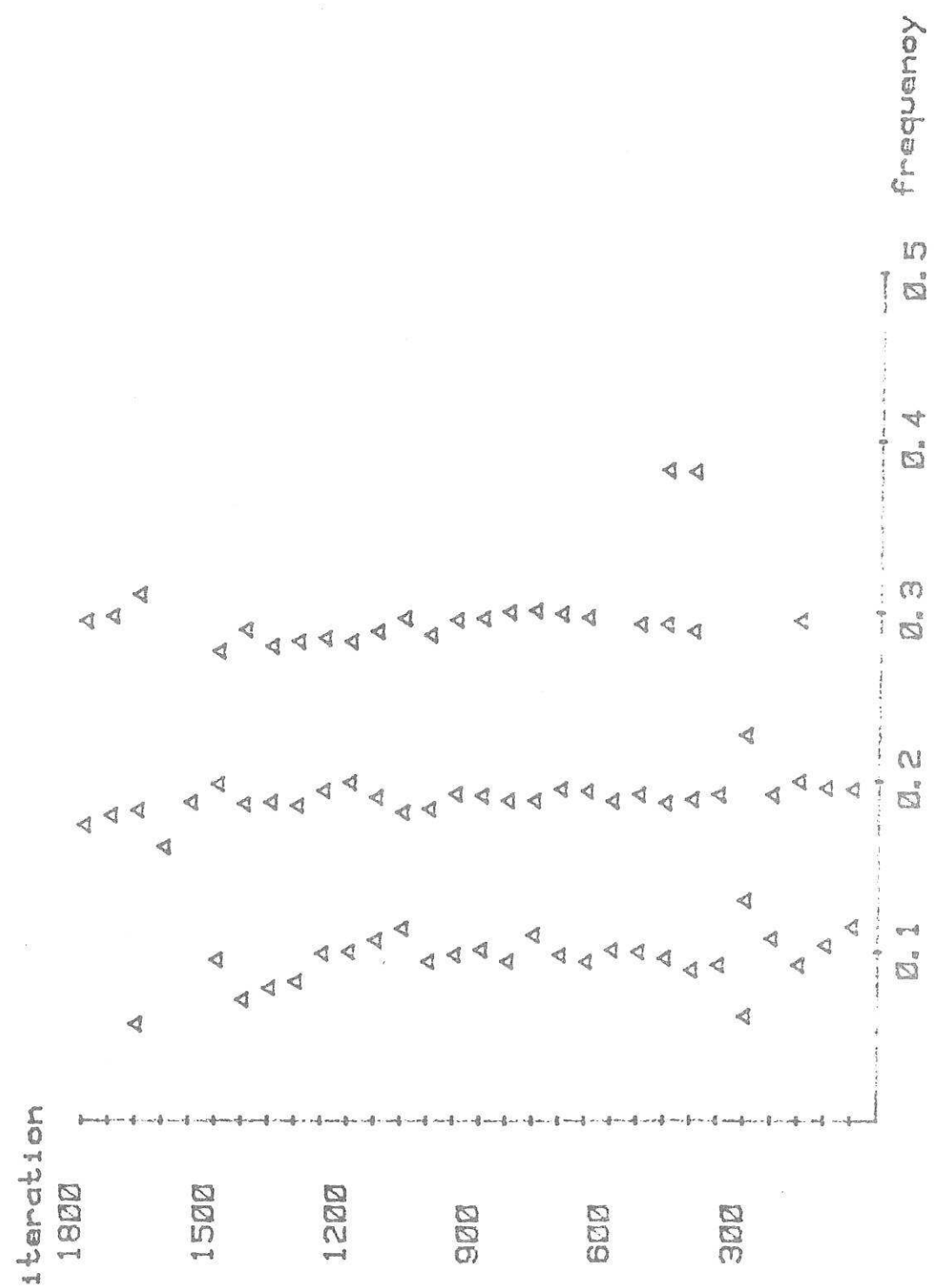
Fig.3

UPPER SURFACE ELECTRODES -- DATA AND FFT :

+5 *10**2

-5

5 *10**8

5

f

1   2   3   4   5
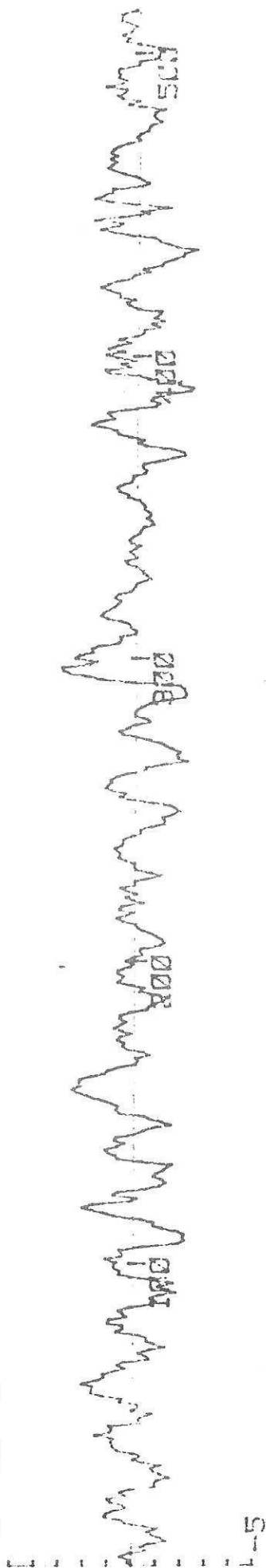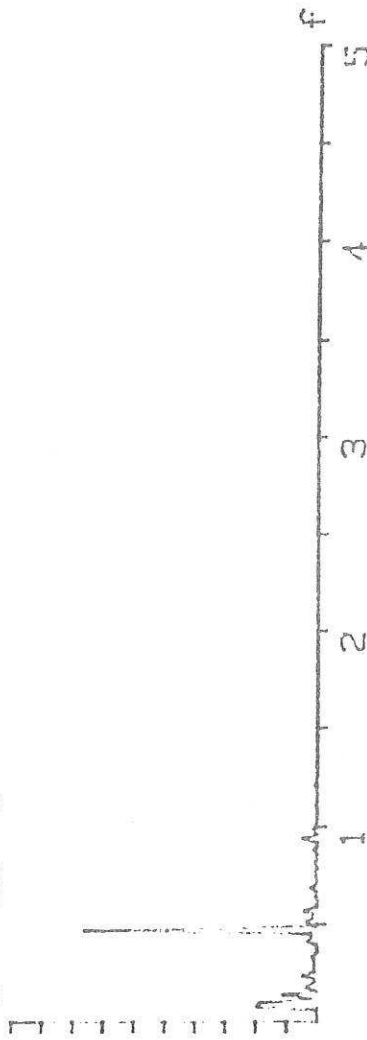
Fig. 4

Fig.5

25TH ORDER MODEL - 13 SAMPLE DELAY
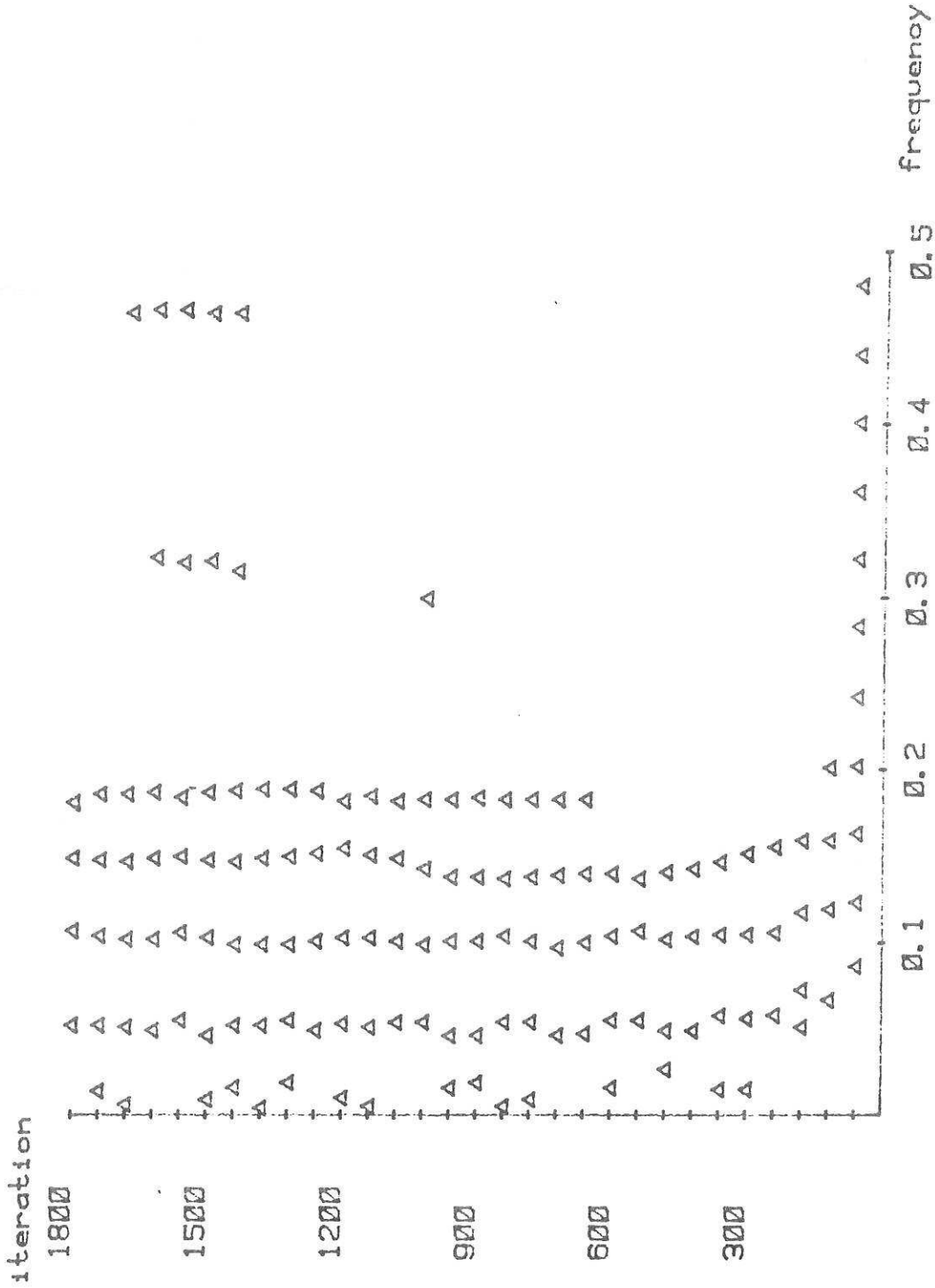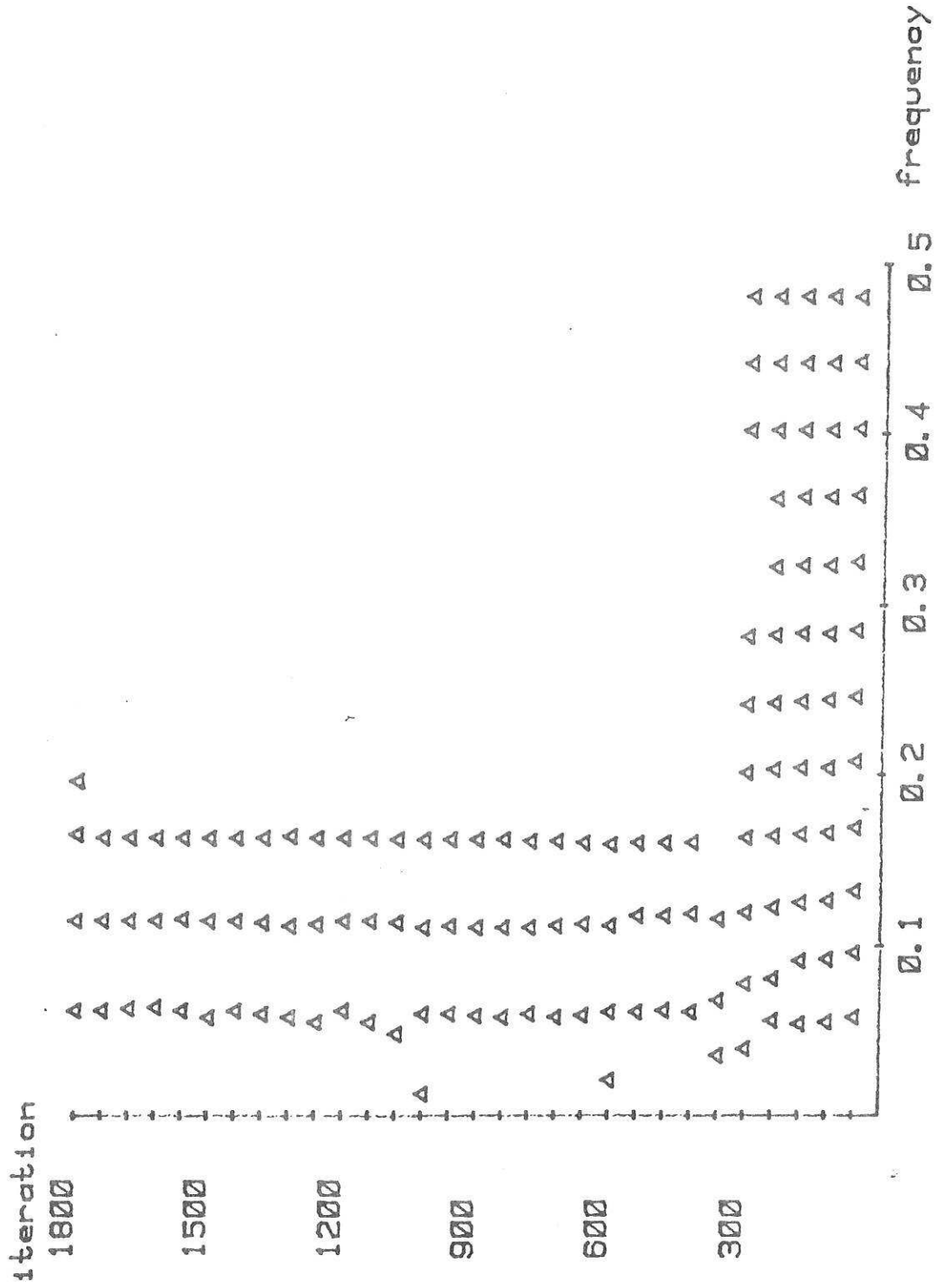
tramp = 1.00 secs - alpha = 0.1661 - tadapt = 150 itns

iteration

1800

1500

1200

900

600

300

0.1   0.2   0.3   0.4   0.5   frequency

tsamp = 1.00 secs — 25TH ORDER FILTER — 13 SAMPLE DELAY ‌
alpha = 0.1661 — tadapt = 150 itns

Fig. 9

tramp = 1.00 secs — 19TH ORDER FILTER — 1 SAMPLE DELAY
— alpha = 0.1659 — tadapt = 114 iths

Fig.7.

teamp = 1.00 secs

25TH ORDER FILTER - 13 SAMPLE DELAY :
- alpha = 0.1661 - tadapt = 150 itns

iteration

1800

1500

1200

900

600

300

0.1   0.2   0.3   0.4   0.5   frequency
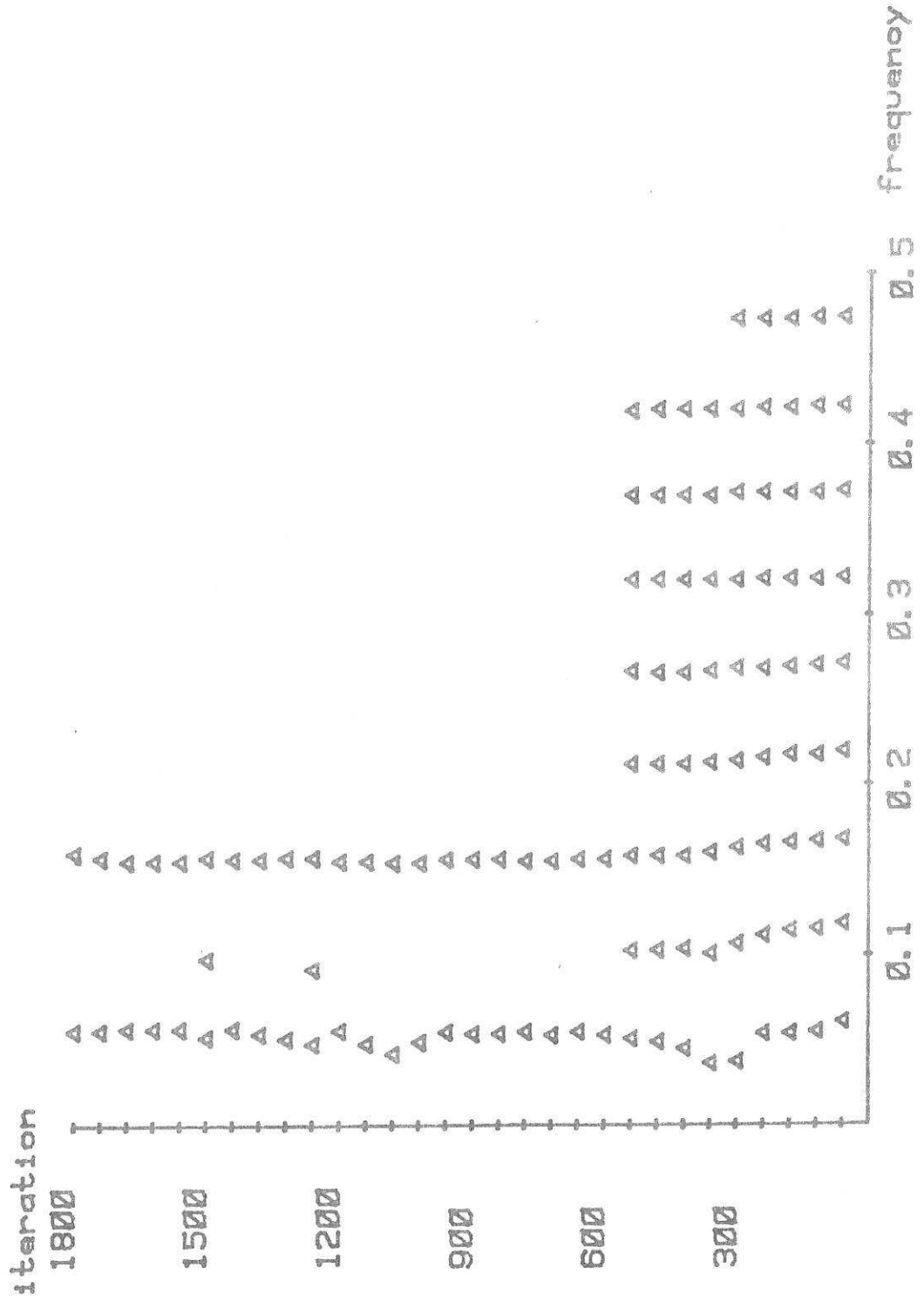
Fig. 8

19TH ORDER FILTER - 1 SAMPLE DELAY -
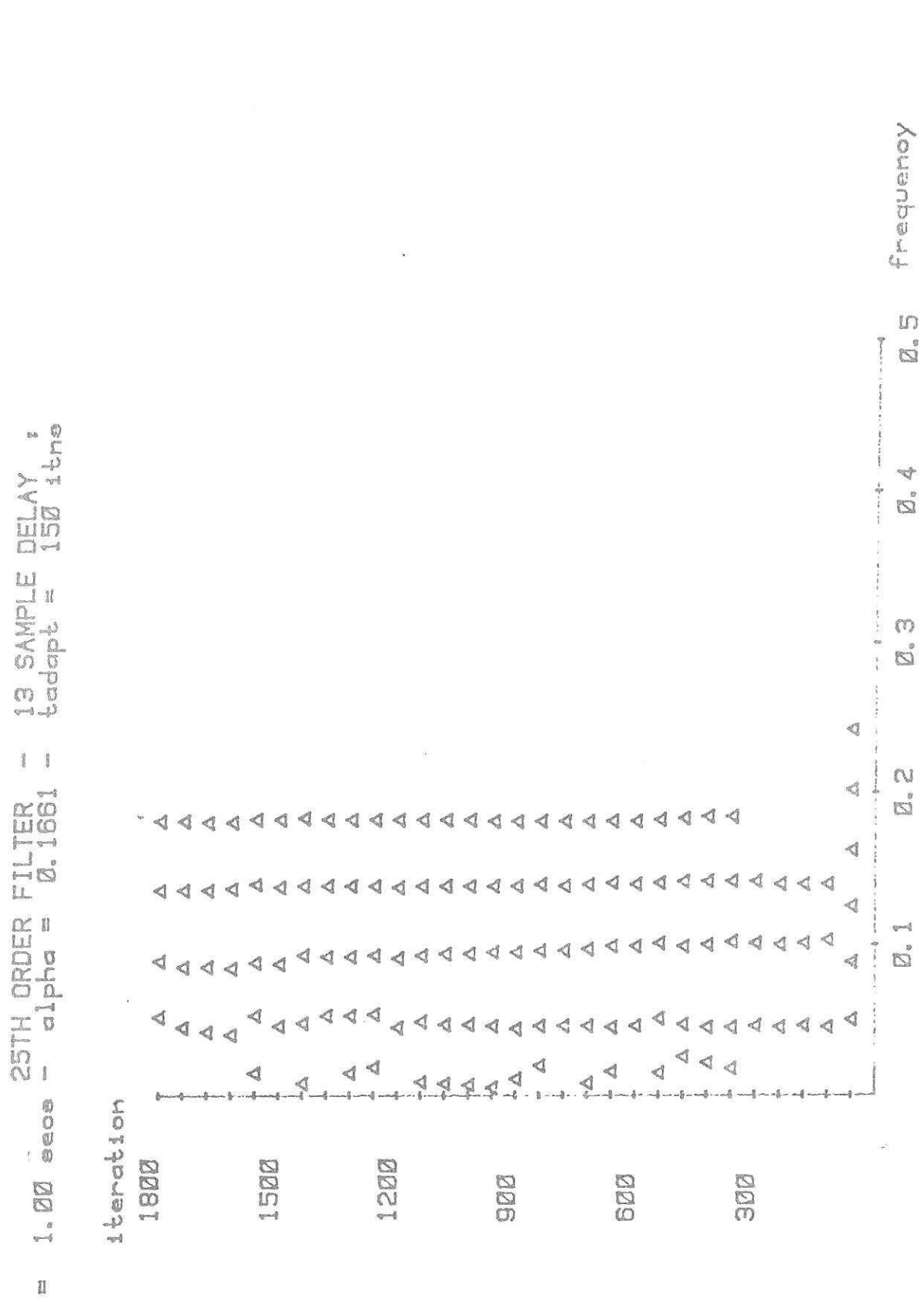
tsamp = 1.00 secs - alpha = 0.1659 - tadapt = 114 itns !

iteration

Fig.9

tsamp = 1.00 secs - alpha = 0.1661 - tadapt = 150 itns

25HT ORDER FILTER - 13 SAMPLE DELAY :

iteration

1800

1500

1200

900

600

300

0.1   0.2   0.3   0.4   0.5   frequency
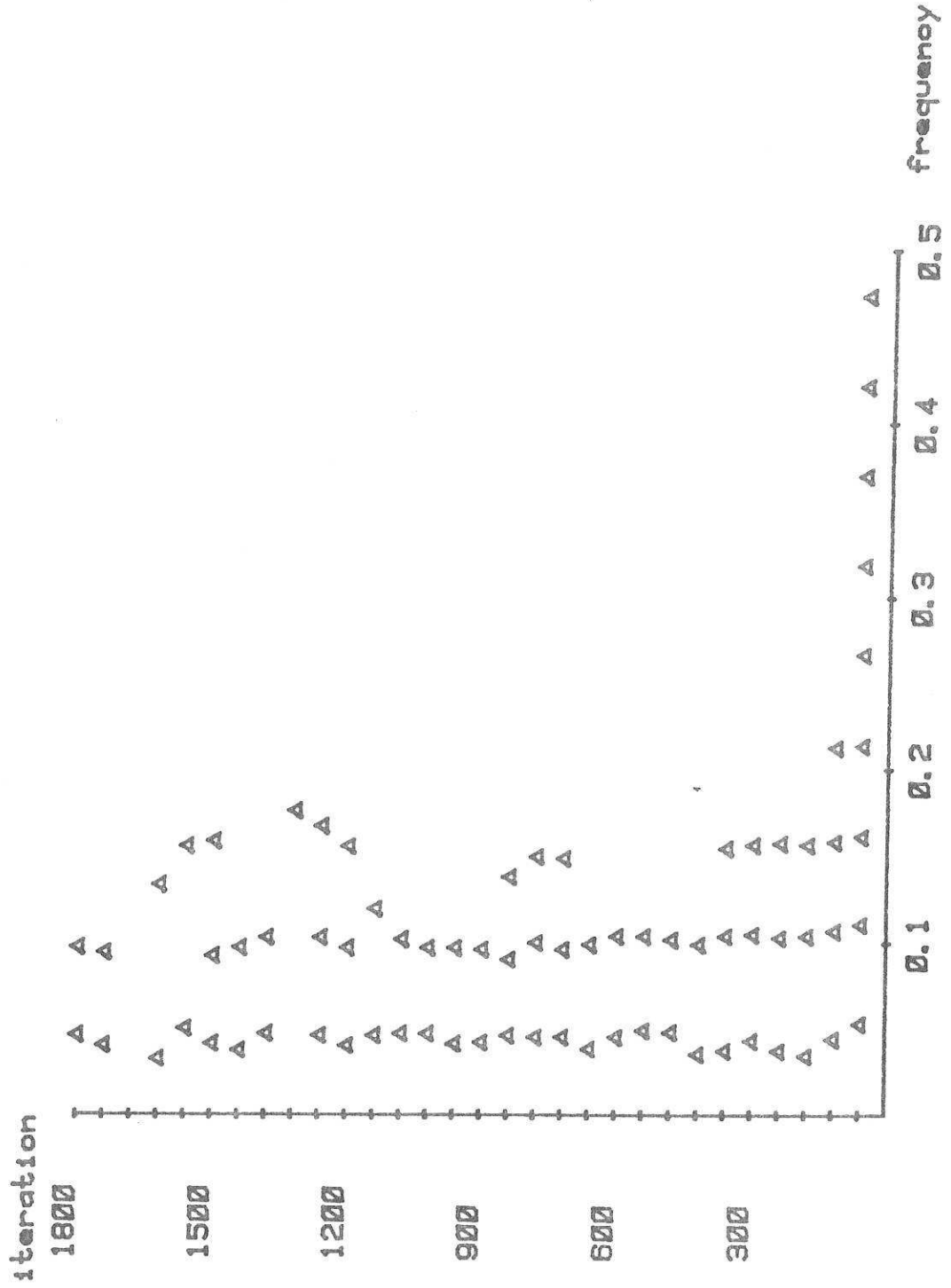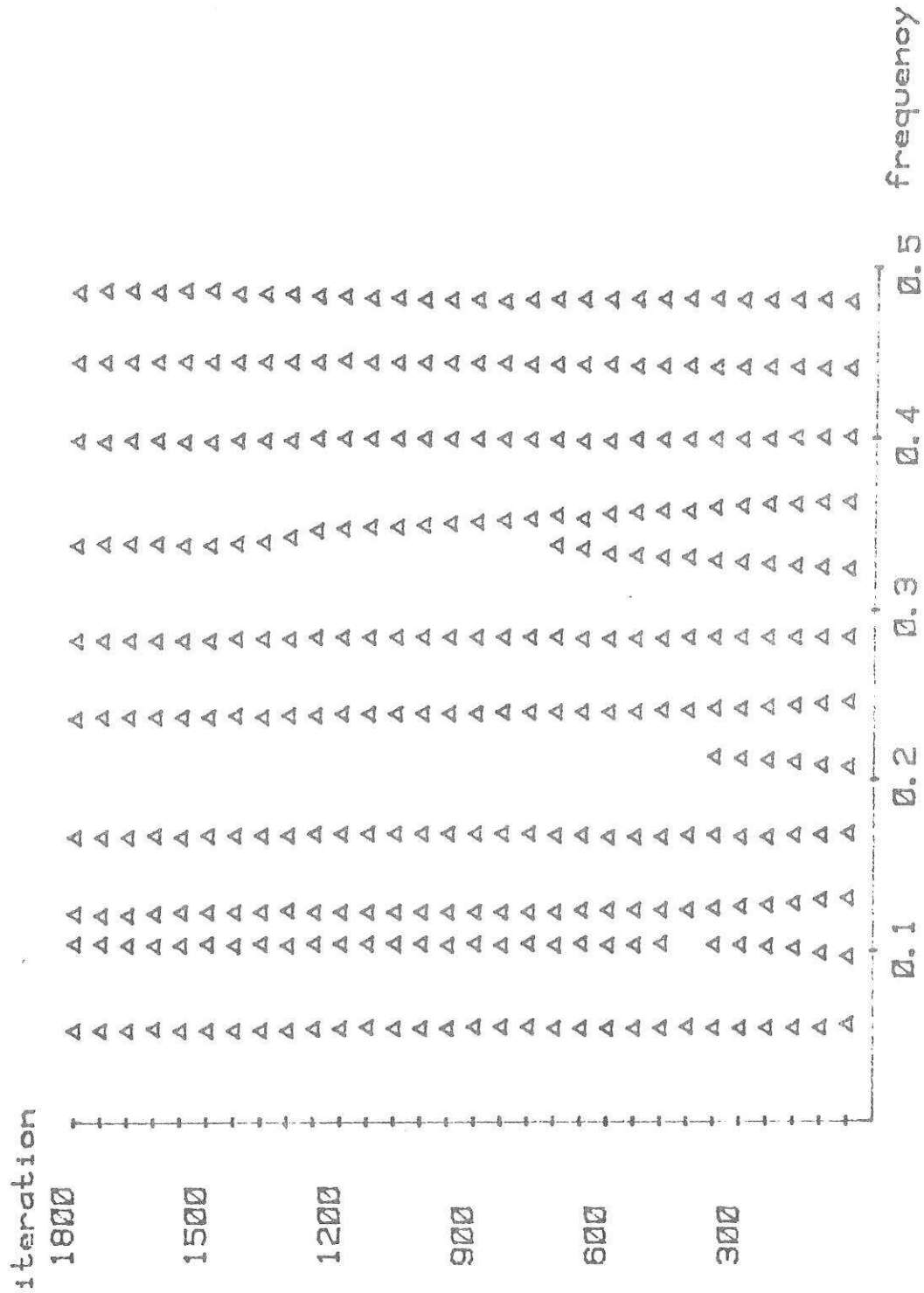
Fig. 10

tcamp = 1.00 secs   25TH ORDER FILTER — 13 SAMPLE DELAY :
                     — alpha = 0.1661 — tadapt = 150 itns
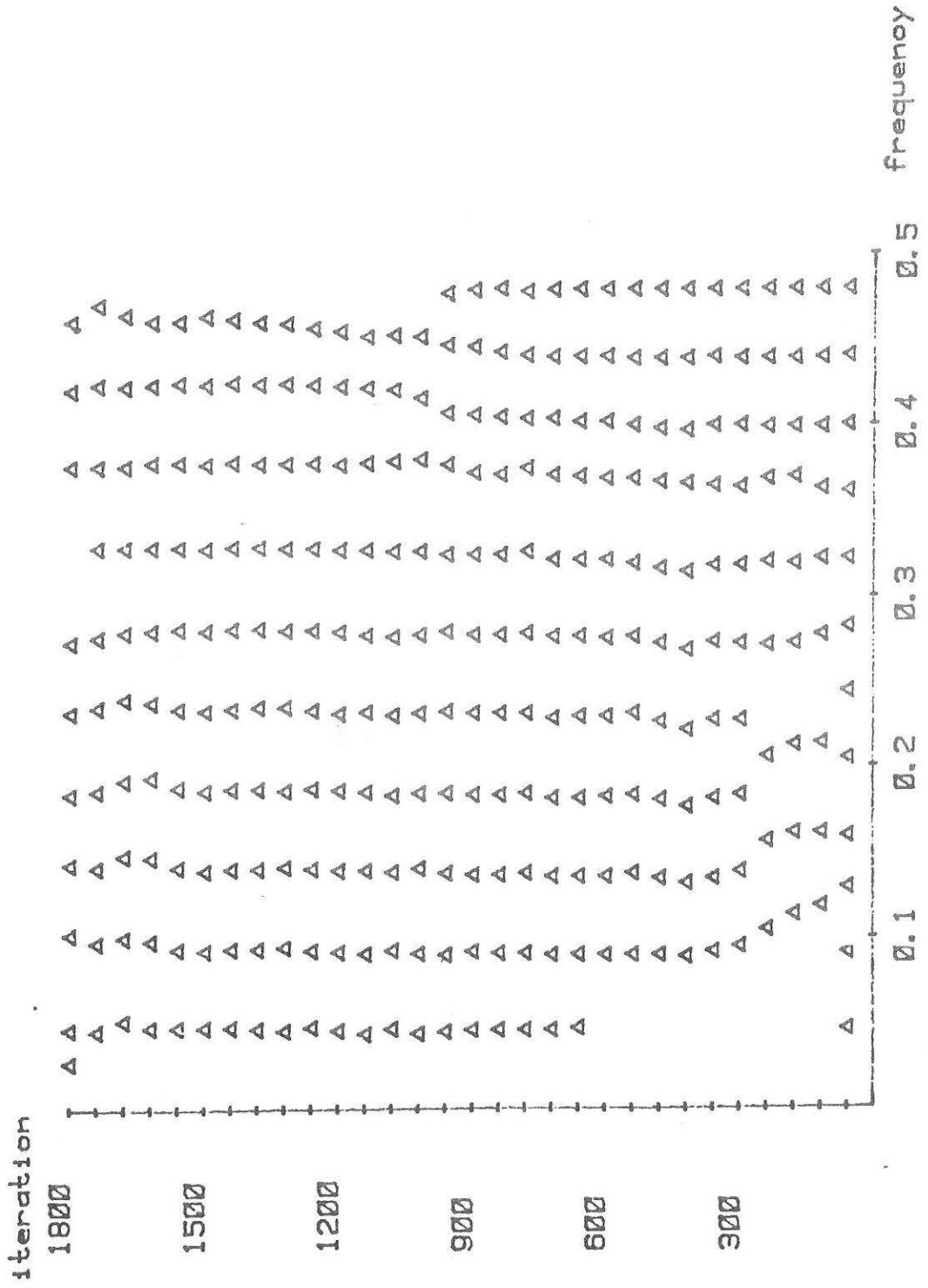
Fig. 11

NASAL GASTRIC TUBE   —   DATA AND FFT :
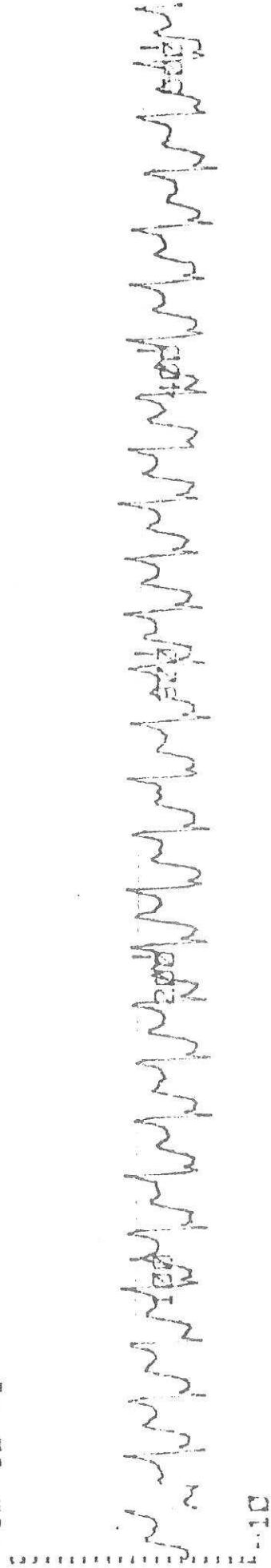
Fig.12
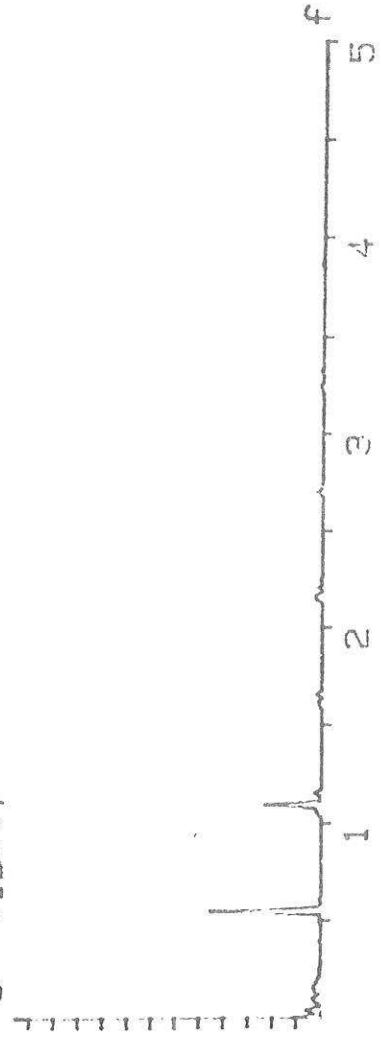
TSAMP = - A L E - 20TH ORDER MODEL
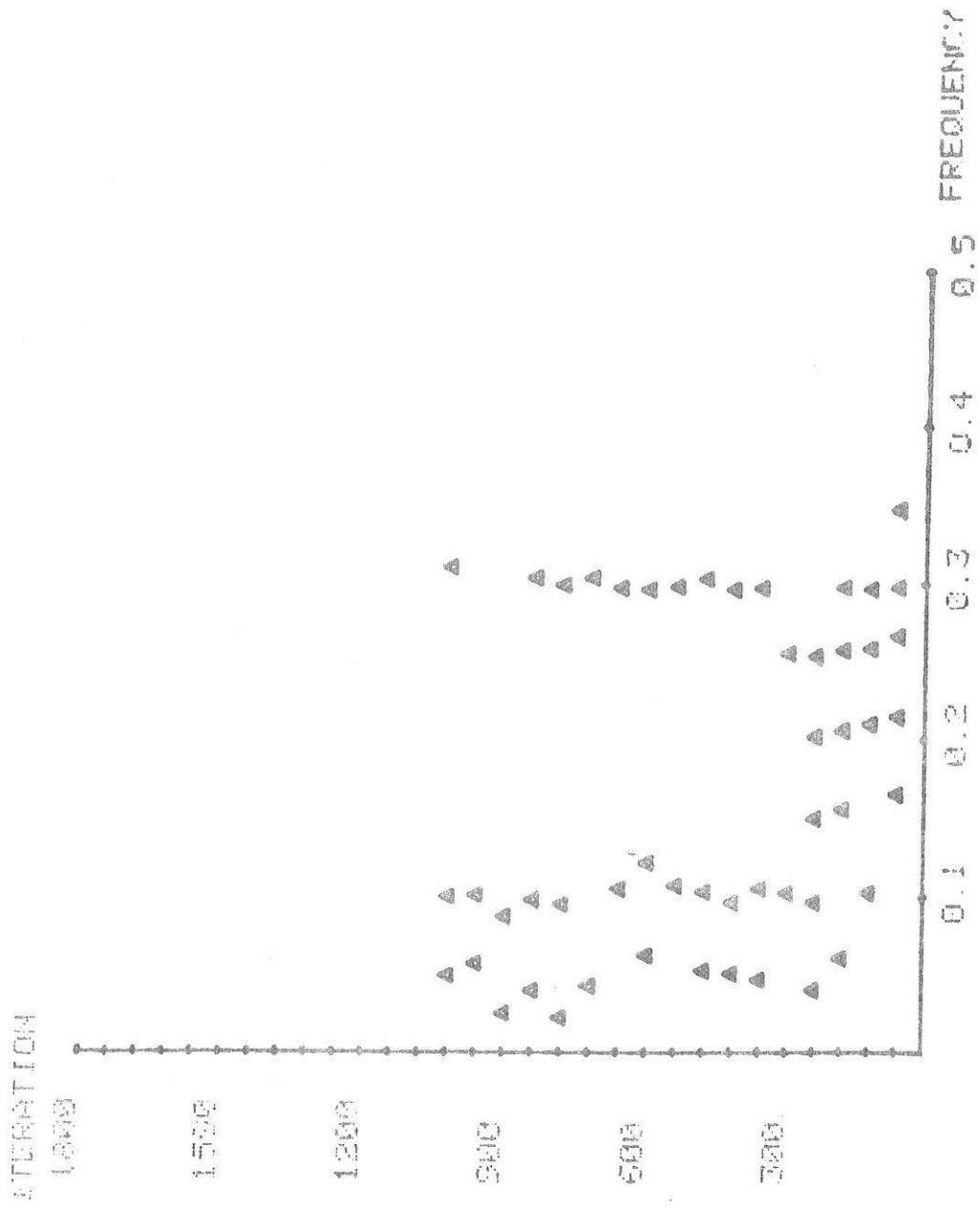= 1.00 SECS - ALPHA = 0.3300 - TADAPT = 60 ITNS

Fig. 13

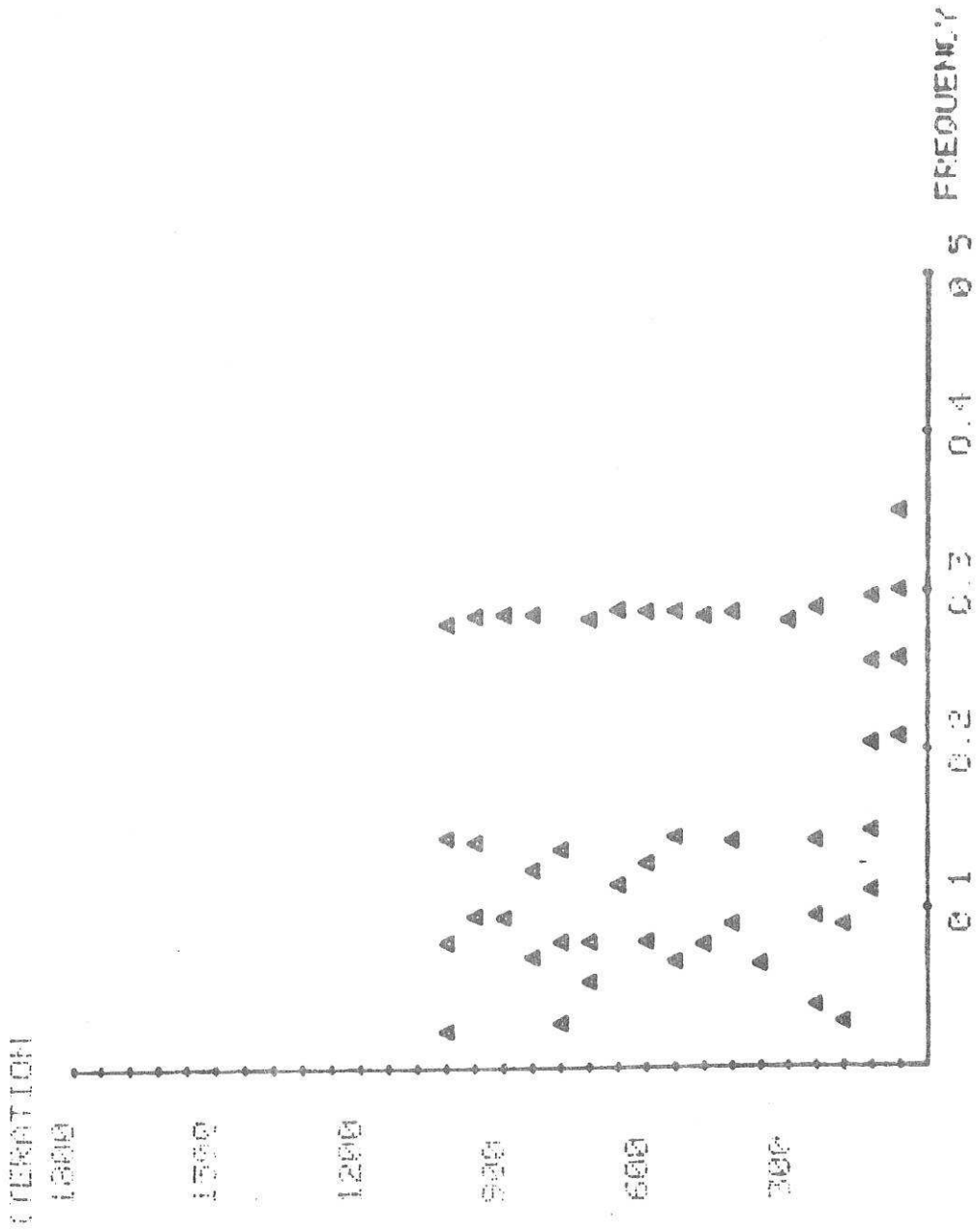TSAMP = 1.00 SECS — A L E — 20TH ORDER MODEL
ALPHA = 0.3300 — TADAPT = 60 ITHS

Fig. 14

TSAMP = - A L E - 20TH ORDER MODEL
= 1.00 SECS - ALPHA = 0.3300 - TAUAFT = 60 ITHS

Fig.15